JCI insight

Patterns of ANA$^+$ B cells for SLE patient stratification

Jolien Suurmond, Yemil Atisha-Fregoso, Ashley N. Barlev, Silvia A. Calderon, Meggan C. Mackay, Cynthia Aranow, Betty Diamond

JCI Insight. 2019;4(9):e127885. https://doi.org/10.1172/jci.insight.127885.

Research Article Immunology

Graphical abstract

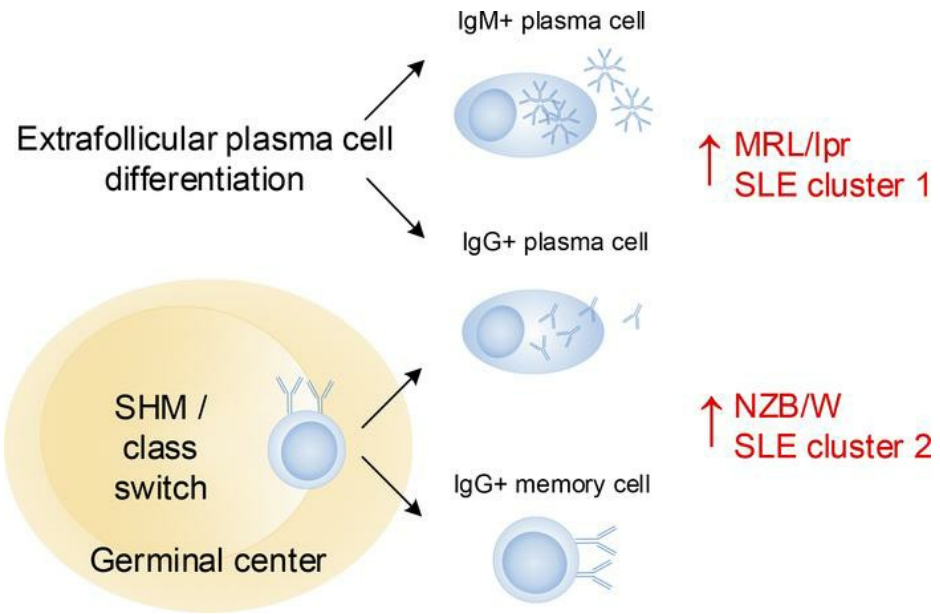

JCI insight

RESEARCH ARTICLE

Patterns of ANA$^+$ B cells for SLE patient stratification

Jolien Suurmond,[1] Yemil Atisha-Fregoso,[1,2] Ashley N. Barlev,[1,3] Silvia A. Calderon,[1] Meggan C. Mackay,[1] Cynthia Aranow,[1] and Betty Diamond[1]

[1]Center of Autoimmune Musculoskeletal and Hematopoietic Diseases, Feinstein Institute for Medical Research, Northwell Health, Manhasset, New York, USA. [2]Tecnologico de Monterrey, Monterrey, Nuevo León, Mexico. [3]Donald and Barbara Zucker School of Medicine at Hofstra/Northwell, Manhasset, New York, USA.

IgG antinuclear antibodies (ANAs) are a dominant feature of several autoimmune diseases. We previously showed that systemic lupus erythematosus (SLE) is characterized by increased ANA$^+$ IgG plasmablasts/plasma cells (PCs) through aberrant IgG PC differentiation rather than an antigen-specific tolerance defect. Here, we aimed to understand the differentiation pathways resulting in ANA$^+$ IgG PCs in SLE patients. We demonstrate distinct profiles of ANA$^+$ antigen-experienced B cells in SLE patients, characterized by either a high frequency of PCs or a high frequency of IgG$^+$ memory B cells. This classification of SLE patients was unrelated to disease activity and remained stable over time in almost all patients, suggesting minimal influence of disease activity. A similar classification applies to antigen-specific B cell subsets in mice following primary immunization with T-independent and T-dependent antigens as well as in lupus-prone mouse models (MRL/lpr and NZB/W). We further show that, in both lupus-prone mice and SLE patients, the classification correlates with the serum autoantibody profile. In this study, we identified B cell phenotypes that we propose reflect an extrafollicular pathway for PC differentiation or a germinal center pathway, respectively. The classification we propose can be used to stratify patients for longitudinal studies and clinical trials.

Introduction

Antinuclear antibodies (ANAs) are present in many patients with autoimmune disease and in essentially all patients with systemic lupus erythematosus (SLE). We and others have shown that B cells reactive with nuclear antigens (ANA$^+$ B cells) are censored during B cell maturation (1–5). This censoring occurs in SLE patients as well as in healthy individuals (1, 2). We previously identified a major tolerance checkpoint for ANA$^+$ IgG$^+$ plasma cells/plasmablasts (hereafter commonly referred to as PCs) in nonautoimmune mice and healthy individuals that is attenuated in SLE patients and in lupus-prone mice (2). In SLE, this correlates with an overall enhanced IgG$^+$ PC differentiation, resulting in an increase in ANA$^+$ IgG PCs in SLE, rather than an antigen-specific selection defect. Although the percentage of IgG PCs that are ANA$^+$ is the same as in healthy controls, there are more IgG PCs in SLE patients.

PCs may arise through 2 main pathways: germinal center (GC) or extrafollicular; both have been implicated in the autoantibody production in SLE (6, 7). GC responses are well known to be increased in lupus-prone mice, and some SLE patients have increased numbers of circulating pre-GC B cells, switched memory B cells and T follicular helper (Tfh) cells, suggestive of enhanced GC responses (8–10). Given that many IgG anti-DNA autoantibodies, which are considered to be pathogenic in SLE, show evidence of somatic hypermutation (SHM) (11), the production of autoreactive PCs by SHM of nonautoreactive naive B cells within the GC has been considered to be an important contributor to the development of SLE in both mice (12) and humans (13) In contrast, extrafollicular PC differentiation in autoimmunity has not been emphasized, although recent studies indicate this pathway may also contribute to SLE (6, 14, 15). MRL/lpr mice exhibit extrafollicular PC generation, although they have increased formation of spontaneous GCs as well (8, 14, 16). In humans, recent research demonstrates that a large proportion of the PCs in some SLE patients are clonally related to naive cells rather than IgG$^+$ memory B cells, suggesting an extrafollicular origin (6).

Conflict of interest: The authors have declared that no conflict of interest exists.

Submitted: January 31, 2019
Accepted: March 19, 2019
Published: May 2, 2019.

Reference information: *JCI Insight*. 2019;4(9):e127885. https://doi.org/10.1172/jci.insight.127885.

Because there are no definitive markers that discriminate PCs based on their pathway of differentiation, it is hard to establish the pathway through which they were derived, especially in humans where access to lymphoid organs is limited. In addition, most studies discriminating extrafollicular responses from GC responses use acute immunization models, and it is not clear if all the paradigms that have been proposed for the distinction between extrafollicular and GC responses apply in the chronic immune activation present in autoimmune conditions.

Here, we aimed to understand the differentiation pathways resulting in ANA$^+$ IgG PCs in SLE patients. Using our flow cytometry–based assay for ANA$^+$ B cells and PCs, we have identified 3 patterns of ANA$^+$ antigen-experienced B cells. We now propose a classification of patients based on the relative frequency of ANA$^+$ memory B cells and PCs.

By correlating this classification with primary immune responses in nonautoimmune mice and the autoimmune response in lupus-prone mice, we identified one pattern that we propose reflects an extrafollicular pathway for PC differentiation and another pattern that reflects a GC pathway. Furthermore, we show that, in the majority of patients, the pattern is stable over time and correlates with antigen recognition by serum autoantibodies.

Results

Distinct phenotypes of ANA$^+$ antigen-experienced B cells in SLE patients. We recently reported that a major B cell abnormality in SLE patients is an increase in total and ANA$^+$ IgG PCs, measured using a flow cytometric assay that determined the frequency of transitional, naive, switched, and unswitched memory cells and IgM and IgG PCs and the proportion of ANA$^+$ cells within each subset (2). Here, we were interested in whether this analysis could help refine our understanding of the differences between healthy subjects and SLE patients and characterize the heterogeneity of SLE patients. We expanded our cohort to 36 SLE patients and confirmed that the frequency of ANA$^+$ IgG PCs and total IgG PCs was significantly increased in SLE patients compared with healthy controls, whereas no significant differences were observed among the other B cell subsets (Figure 1, A–F, and Supplemental Figure 1, A–D; supplemental material available online with this article; https://doi.org/10.1172/jci.insight.127885DS1). Demographic characteristics of the SLE patients and healthy subjects were not significantly different, except for ethnicity (Supplemental Table 1). We observed a large spread in the frequency of ANA$^+$ IgG PCs in SLE patients. A proportion of patients (~40%) did not demonstrate increased frequencies of ANA$^+$ IgG PCs compared with healthy subjects (using a nonparametric cutoff for the frequency of ANA$^+$ IgG PCs in healthy subjects (quartile 3 + 1.5 × interquartile range within the healthy subjects) (Figure 1E). We designated these patients as cluster 0.

We performed a principal component analysis, based on all flow cytometry B cell parameters studied (percentages of total and ANA$^+$ transitional, naive, IgG memory, IgM, and IgG PCs) to analyze clustering of SLE patients and healthy subjects in a nonbiased way and to see if we could use these parameters to stratify the SLE patients (Figure 1, G and H). Cluster 0 patients, without PC expansion, overlapped largely with the healthy controls (Figure 1, G and H). The cluster 0 phenotype was not related to clinical parameters such as disease activity or medication (Supplemental Table 2). Although there are no suggestions of active ongoing ANA$^+$ PC differentiation in blood of individuals within cluster 0, the proportion of patients with anti-dsDNA positivity and the range of anti-DNA titers was similar to that of the patients with circulating PC expansion, suggesting that serum autoantibodies in cluster 0 may be derived from long-lived PCs residing in the bone marrow or other tissues. To understand pathways of PC differentiation in SLE, we next focused on SLE patients with significantly higher numbers of circulating ANA$^+$ PCs.

The frequencies of ANA$^+$ and total IgM and IgG PCs all contributed strongly to principal component 1 (Figure 1G), which was the main discriminator for SLE patients without or with PC expansion (Figure 1H). Another main contributor to principal component 1 was the IgG$^+$ memory B cell subset (Figure 1G). Importantly, in SLE patients with an expansion of ANA$^+$ IgG PCs, the memory B cells and PCs are present in inverse frequency, such that the patients with the highest ANA$^+$ PC numbers generally have lower numbers of ANA$^+$ memory B cells and vice versa, leading to opposing vectors for PCs and memory B cells in the principal component analysis (Figure 1, G and I). To assess these 2 groups of patients and enable a classification paradigm, patients were grouped based on ANA$^+$ IgM and IgG PCs relative to ANA$^+$ memory B cells. A 20% cutoff for the relative proportion of ANA$^+$ PCs among ANA$^+$ antigen-experienced B cells (PCs and memory cells) was chosen to distinguish cluster 1 (>20% ANA$^+$ PCs compared with ANA$^+$ IgG memory B cells) from cluster 2 (<20% ANA$^+$ PCs compared with ANA$^+$ IgG memory B cells) (Figure 1J).

Using this cutoff, the principal component analysis showed a separation of the 2 groups of patients with expansion of circulating ANA$^+$ PCs (Figure 1K). Approximately one-third of the patients with an expansion of ANA$^+$ PCs showed a cluster 1 phenotype, whereas the remaining two-thirds of the patients belonged to cluster 2.

Interestingly, although it has been reported that patients with active disease have increases in total PC frequency (17), the clustering seemed independent of SLE disease activity index (SLEDAI) scores, which overlapped in all 3 groups (Figure 1J and Supplemental Table 2), and we did not observe a correlation of SLEDAI with the frequency of total IgG PCs or ANA$^+$ IgG PCs (data not shown). Furthermore, when including only patients with active disease (SLEDAI >4), the same clustering was observed (data not shown). Patients from cluster 2 were less likely to be on steroids (Supplemental Table 2), although each cluster contained patients that did not use this medication.

There is a conflict in the literature as to whether SLE autoreactivity is a consequence of activation of naive cells into PCs directly through an extrafollicular pathway or via activation of a GC response with generation of both memory B cells and PCs. Our data suggest that there are 2 clusters of SLE patients with an expanded proportion of PCs, 1 of which has a high and 1 a low frequency of ANA$^+$ memory B cells. We believe that a cutoff of 20% although arbitrary, provides a simple method to define and classify patients based on the relative proportions of ANA$^+$ antigen-experienced B cell subsets.

Phenotype of ANA$^+$ B cells and PCs in SLE patients is stable over time. Clinical data suggested that there is no clear correlation of the cellular phenotypes with disease activity, or other patient characteristics, except steroid use; nonetheless, we sought to establish the stability of the classification over time. This is particularly important, as T-dependent immune responses, such as in response to vaccination or infection, are usually characterized by an initial wave of PCs derived from an extrafollicular response, followed by GC response with IgG$^+$ memory B cells and PCs. Therefore, a response that is characterized initially by large numbers of PCs might develop into a response dominated by memory B cells over time, in particular when the initial analysis is done during a clinical flare. Using our classification paradigm, 13 patients were reassessed between 1 and 12 months after their initial assessment (Figure 2A). Of the 5 patients from cluster 1 that were analyzed twice, 4 remained in this cluster over a time period ranging from 2 months to 1 year, demonstrating that individuals in this cluster do not routinely progress to a cluster 2 classification. Of the 6 patients from cluster 2 with repeat analyses occurring from 1 month to 1 year, 5 showed the same classification. Two patients in cluster 0 were analyzed a second time and both maintained the same ratio of memory to PCs. Furthermore, using the principal components identified in Figure 1 to analyze the repeat assessments showed similar clustering of the individual patients (Figure 2B). Even the 2 patients whose classification based on the relative frequency of ANA$^+$ PCs relative to ANA$^+$ memory cells changed (black dotted arrows) generally fell within the same area on the principal component analysis plot (Figure 2B). Importantly, all patients with considerable changes in disease activity (change in SLEDAI ≥5) (SLE 01, SLE 05, SLE 25, SLE 32) and clinical features of disease (SLE 01, SLE 05, SLE 07, SLE 25) and all patients who had a flare during one of the measurements (SLE 05, SLE 07, SLE 32), except one (SLE19), retained the same classification, and almost all subjects with a considerable change in medications (SLE 01, SLE 05, SLE 07, SLE 09, SLE 25, SLE 32) also preserved their cluster classification (Figure 2A and Supplemental Table 3). Two patients in cluster 2 started using PDN (SLE 01, SLE 09), but each retained the same classification, suggesting that the more frequent use of PDN in cluster 1 patients was not directly affecting their clustering.

These data suggest that although the classification scheme is necessarily arbitrary, the vast majority of patients (85%) show stability of their classification, further confirming the robustness of our ANA assay. Moreover, the relative proportions of autoreactive memory B cells and PCs in SLE patients seems imprinted, possibly by genetic risk factors.

Classification paradigm in prototypical GC and extrafollicular responses in mice. We next wanted to study how the frequencies of memory B cells and PCs would relate to prototypical immune responses. Several characteristics are known for extrafollicular and GC responses in mice (Figure 3A): extrafollicular responses are usually characterized by a high number of PCs in the absence of IgG$^+$ memory B cells, whereas GC responses are characterized by class-switched PCs and memory B cells. We therefore wanted to test if our classification method that we used in SLE patients can distinguish these responses based on frequencies of antigen-specific B cells following immunization. We immunized wild-type C57BL/6 mice with the T-independent antigen 4-Hydroxy-3-nitrophenylacetyl-Ficoll (NP-Ficoll) and the T-dependent

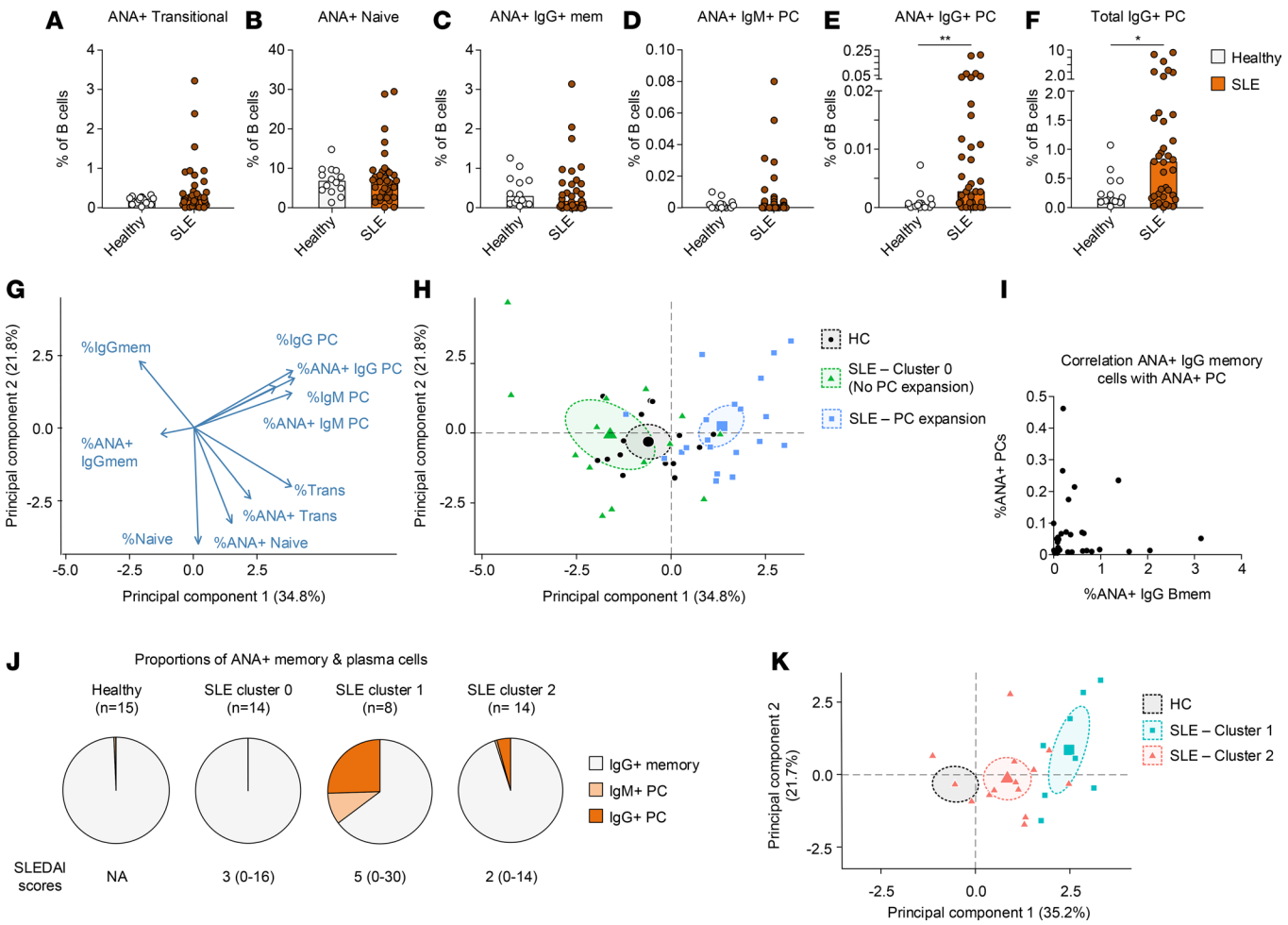

Figure 1. Distinct phenotypes of ANA⁺ B cells and PC in SLE patients. (**A**–**F**) Frequencies of ANA⁺ and total B cell subsets in healthy controls (n = 15) and SLE patients (n = 36). Each dot indicates an individual, and the bars represent the median. *P < 0.05; **P < 0.01, using Mann-Whitney test. (**G** and **H**) Principal component analysis of all B cell parameters analyzed (frequencies of ANA⁺ and total B cell and PC subsets). The percentage indicated on the axis is the percentage of variance explained by that principal component. SLE patients were separated based on whether they displayed an increase in the frequency of ANA⁺ IgG PCs compared with healthy controls (quartile 3 + 1.5 × interquartile range). Patients without expansion are denoted as "cluster 0." (**G**) The variables contributing to each dimension in principal component analysis. The length and direction of each arrow shows the strength of their contribution to each PC. (**H**) The coordinates of each healthy individual and SLE patient. Ellipses represent the 95% confidence interval for each group. (**I**) Frequency of ANA⁺ IgG⁺ memory B cells and ANA⁺ PCs in SLE patients with an expansion of ANA⁺ PCs. Each dot indicates a patient (n = 22). (**J**) Relative proportion of ANA⁺ IgG memory B cells and ANA⁺ IgM and IgG PCs in healthy controls and SLE patients. The median and range of SLEDAI scores is shown below each circle. Patients were defined as "cluster 1" when their ANA⁺ PCs were >20% of the total ANA⁺ antigen-experienced cells (memory B cells and PCs). Patients were defined as "cluster 2" when their ANA⁺ PCs were <20% of the total ANA⁺ antigen-experienced cells. (**K**) Principal component analysis as in **C** and **D**, here only showing patients from cluster 1 and 2. ANA, antinuclear antibody; HC, healthy control; PC, plasmablast/plasma cell; SLE, systemic lupus erythematosus; SLEDAI, SLE disease activity index.

antigen nitrophenylated–chicken γ globulin (NP-CGG). We analyzed NP-Ficoll–immunized mice at day 7 and NP-CGG–immunized mice at day 7, 14, and 21. NP-Ficoll induces an extrafollicular response, and NP-CGG induces a T-dependent response with the generation of PCs through a T-dependent extrafollicular pathway on day 7 and PC generation through the GC on day 14 and 21 (18–20). We analyzed antigen-specific NP⁺ IgG⁺ GC B cells, NP⁺ IgG⁺ non-GC B cells ("switched memory B cells"), and NP⁺ PCs (separated for cytoplasmic IgM and IgG) following immunization (Figure 3B). As expected, NP⁺ IgG⁺ GC B cells were present only following immunization with NP-CGG (Figure 3, C–F). The generation of extrafollicular IgM and IgG NP⁺ PCs had similar kinetics with a peak of NP⁺ PCs on day 7. To characterize each response with respect to the clusters we observed for ANA⁺ B cells in SLE patients, we analyzed the proportions of antigen-specific IgG⁺ non-GC (memory) cells, IgM⁺ PCs, and IgG⁺ PCs (Figure 3G). We observed that the pattern of NP⁺ antigen-experienced cells in the extrafollicular response following NP-Ficoll (day 7) and NP-CGG (day 7) was characterized by a dominant PC phenotype, with only a few IgG⁺ memory B cells.

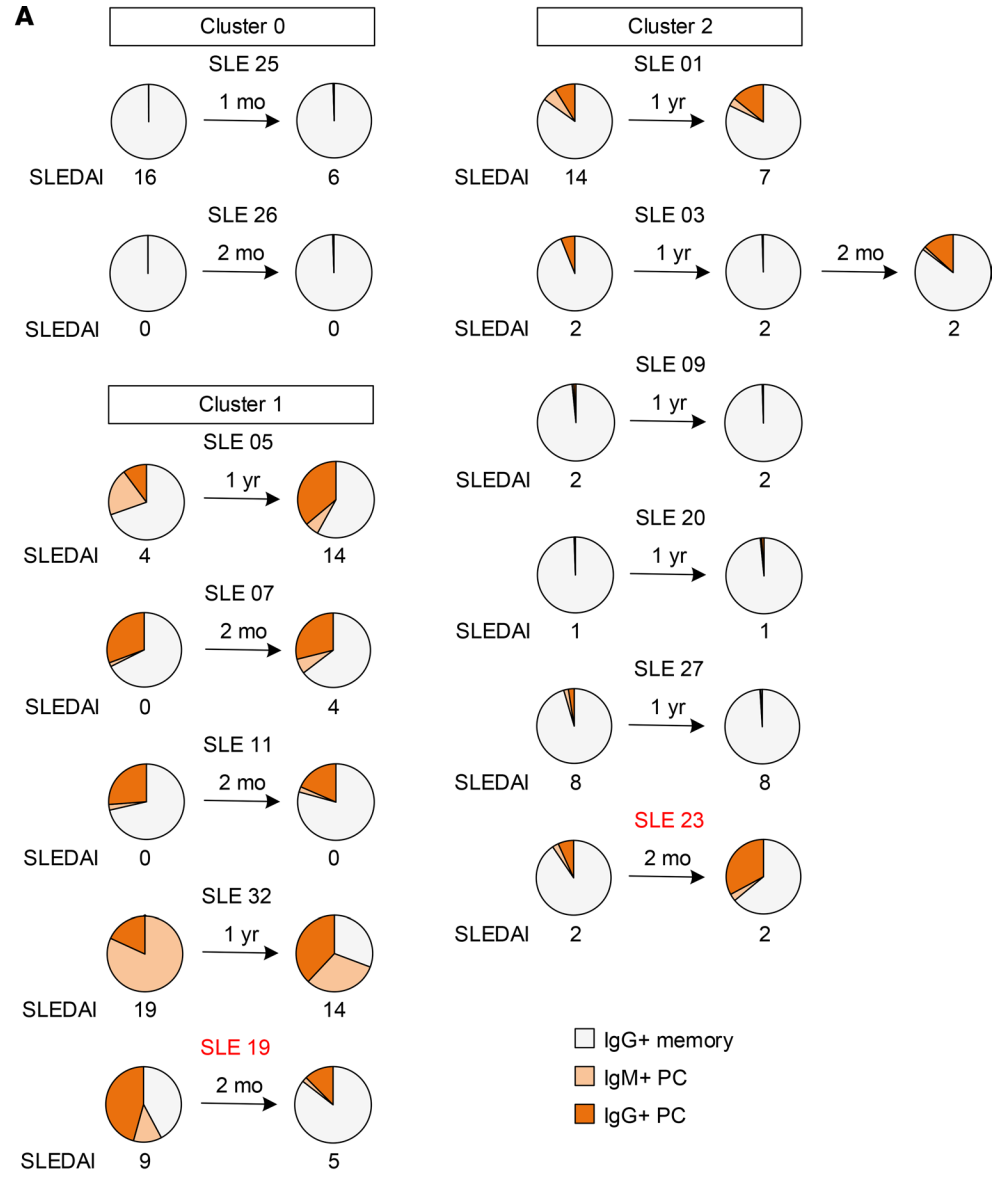

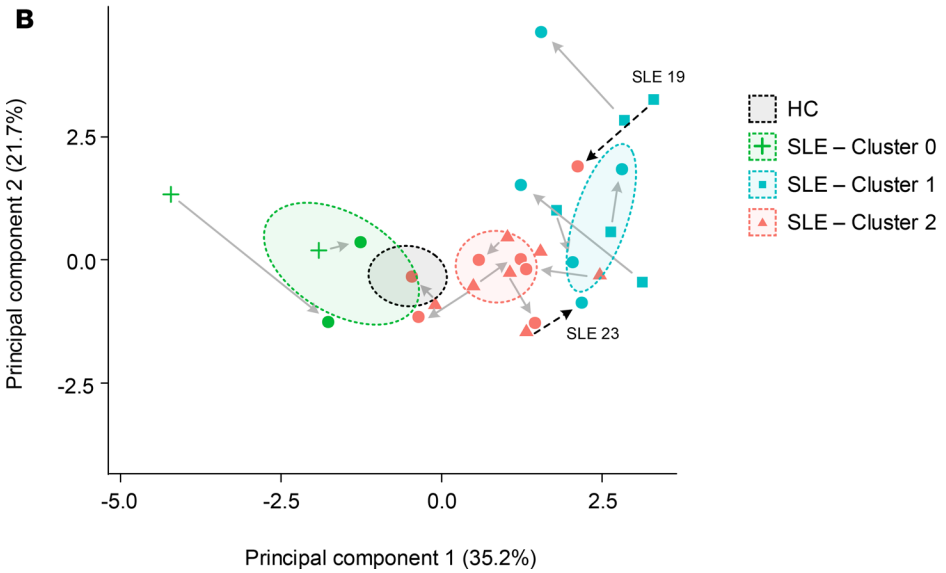

Figure 2. Stability of clustering over time. SLE patients were classified as described in Figure 1, and a follow-up was done between 1 month and 1 year. (**A**) Relative proportion of ANA$^+$ IgG memory B cells and ANA$^+$ IgM and IgG PCs in healthy controls and SLE patients. The SLEDAI scores at the time of each measurement are shown below each circle. Patients indicated in red had a change in classification between the first and second assessment. (**B**) Principal component analysis as in Figure 1, including all initial measurements for healthy subjects and patients, was used to predict the follow-up measurements in each patient. Individual dots represent only those patients with a follow-up measurement. Arrows indicate the follow-up measurement. Dotted black arrows indicate 2 patients (SLE 19 and SLE 23) for whom the classification based on the proportions in **A** changed over time. ANA, antinuclear antibody; HC, healthy control; PC, plasmablast/plasma cell; SLE, systemic lupus erythematosus; SLEDAI, SLE disease activity index.

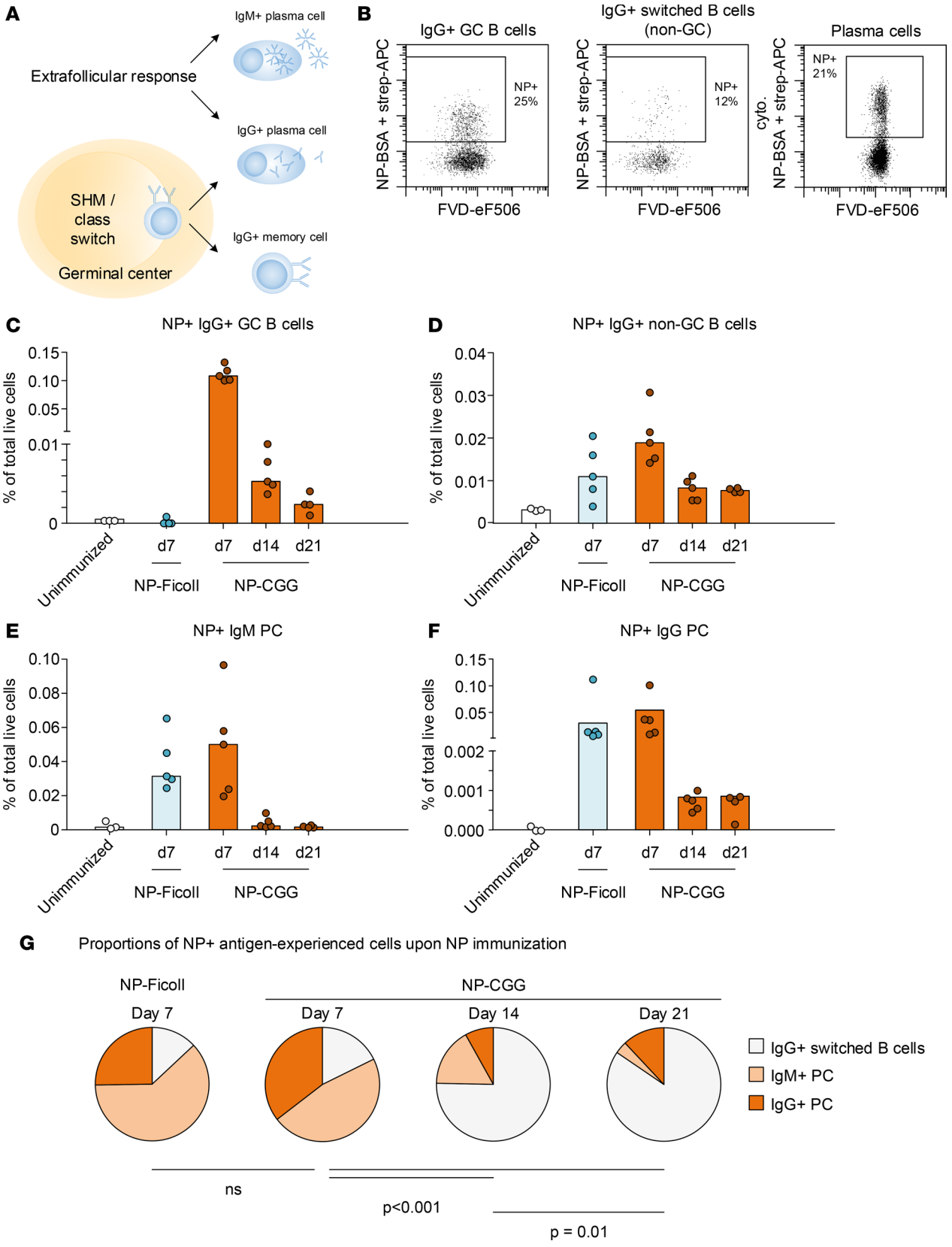
A
IgM+ plasma cell
Extrafollicular response
IgG+ plasma cell
SHM / class switch
Germinal center
IgG+ memory cell
B
IgG+ GC B cells
IgG+ switched B cells (non-GC)
Plasma cells
NP-BSA + strep-APC
cyto. NP-BSA + strep-APC
FVD-eF506
NP+ 25%
NP+ 12%
NP+ 21%
C
NP+ IgG+ GC B cells
D
NP+ IgG+ non-GC B cells
% of total live cells
Unimmunized
d7
d7
d14
d21
NP-Ficoll
NP-CGG
E
NP+ IgM PC
F
NP+ IgG PC
G
Proportions of NP+ antigen-experienced cells upon NP immunization
NP-Ficoll
NP-CGG
Day 7
Day 7
Day 14
Day 21
IgG+ switched B cells
IgM+ PC
IgG+ PC
ns
p<0.001
p = 0.01

Figure 3. Frequencies of memory B cells and PCs upon primary immunization in mice. (**A**) Model for differentiation of PCs. Two pathways can result in the differentiation of ANA$^+$ IgG$^+$ PCs, extrafollicular and germinal center, each leading to different proportions of IgG$^+$ memory cells, IgM PCs, and IgG PCs. (**B**–**G**) C57BL/6 mice were immunized with NP-Ficoll or NP-CGG and analyzed at day 7, 14, and 21 after immunization. (**B**) Representative flow cytometry plots showing the frequency of NP$^+$ cells among GC B cells, memory B cells, and PCs (the latter was analyzed upon cytoplasmic staining for NP). (**C**–**F**) Frequencies of NP$^+$ GC B cells, NP$^+$ memory B cells, NP$^+$ IgM PCs, and NP$^+$ IgG PCs. Each dot shows an individual mouse, and the bar represents the median. (**G**) Proportion of NP$^+$ memory B cells and PCs These were calculated after subtracting the number of NP-specific cells in each population in unimmunized mice. Each pie chart shows the median for each strain (n = 4–6 mice per group). P values were calculated using χ^2 test. ANA, antinuclear antibody; CGG, chicken γ globulin; FVD, fixable viability dye; GC, germinal center; NP, 4-hydroxy-3-nitrophenylacetyl; PC, plasmablast/plasma cell; SHM, somatic hypermutation.

In contrast, the GC response on day 14 and 21 induced by immunization with NP-CGG was characterized by a major decrease in the ratio of PCs to memory B cells. These data demonstrate that relative frequencies of antigen-specific memory and PCs correlate with an extrafollicular or GC origin.

Classification of memory B cells and PCs in lupus mice. As the frequencies of memory B cells and PCs in a primary immunization are to a large degree defined by the kinetics of the response, which do not necessarily display the same characteristics as a chronic autoimmune response, we next sought to analyze the relative frequencies of autoreactive antigen-experienced cells in 2 well-studied lupus mouse models, MRL/lpr and NZB/W mice, with chronic B cell activation. Our previous data showed that both of these mouse strains are characterized by increased frequencies of ANA$^+$ IgG PCs (2), similar to SLE patients. These mouse models are well known to have dominant G activation (NZB/W) or extrafollicular PC differentiation (MRL/lpr), respectively (14, 16, 21–23), NZB/W mice develop autoantibodies at a later time point than MRL/lpr mice (2). We therefore analyzed NZB/W mice before (age 3 months) and after (age 6 months) seroconversion to IgG anti-DNA reactivity to determine whether the pattern of antigen-specific cells would change around the time that autoantibodies develop. Seropositive NZB/W mice had an increase in ANA$^+$ IgG$^+$ switched B cells coincident with a change in PC phenotype from IgM to IgG compared with young mice, which only had an increase in IgM$^+$ PCs (Figure 4A). In contrast, the pattern of ANA$^+$ antigen-experienced cells in MRL/lpr mice was very distinct with a large increase in ANA$^+$ PCs with only few IgG$^+$ switched B cells. Although the relative frequency of ANA$^+$ IgM PCs in NZB/W mice was more than 20% of antigen-experienced cells, the change at the time of seroconversion from young to old mice showed a dominant ANA$^+$ IgG$^+$ memory B cell compared with PC frequency (Figure 4A, right circle).

These different frequencies of ANA$^+$ memory B cells and PCs are similar to what was observed following immunization with NP and analogous to what we observed in SLE patients.

Distinct IgG isotype usage, autoantibody affinity, and antigen recognition profiles characterize MRL/lpr versus NZB/W mice. IgG3 antibodies are characteristic of T-independent extrafollicular responses (24, 25). We, therefore, explored IgG isotypes in ANA$^+$ PCs from MRL/lpr and NZB/W mice and from mice immunized with NP-Ficoll and NP-CGG. There was an increase in the frequency of ANA$^+$ IgG3$^+$ PCs in MRL/lpr mice compared with NZB/W mice (Figure 4, B–D). The IgG3 anti-dsDNA titer was also increased in MRL/lpr mice (Figure 4E), as has been reported in the literature (26, 27), consistent with the increase in ANA$^+$ IgG3$^+$ PCs we observed. The relative frequency of IgG3 over the other IgG isotypes (IgG1, 2a/c, and 2b) was increased in MRL/lpr mice compared with NZB/W mice (Figure 4, F and G), a pattern that correlated with the T-independent response to NP-Ficoll (Figure 4, H and I).

We next asked whether our classification paradigm correlates to other parameters that can be measured in serum, in particular ones that could be studied in humans as well. If the ANA$^+$ PCs arise from different PC differentiation pathways in the 2 lupus-prone strains, we might expect to see a difference in affinity of autoantibodies and the spectrum of their specificities. We first determined the relative affinity of anti-dsDNA antibodies by inhibition ELISA. We observed a higher IC_{50} in IgG anti-dsDNA from MRL/lpr mice compared with NZB/W mice, suggesting that the relative affinity in MRL/lpr mice is lower (Figure 5, A and C). Importantly, no difference was observed in the relative affinity of IgM anti-dsDNA antibodies between the 2 strains (Figure 5, B and D). In addition to affinity and IgG subclass, we also analyzed the ANA specificity profile of serum IgG and IgM, as extrafollicular antibodies may bind to a broader array of antigens. We used hierarchical clustering to analyze whether a nonsupervised clustering would independently show a difference between these strains. Antigen recognition by IgG from serum of these lupus-prone mice clustered by strain (except for 1 NZB/W mouse) (Figure 5E), with IgG from MRL/lpr mice recognizing an increased number of antigens compared with IgG from NZB/W mice (Figure 5F). In contrast, the IgM profile did not cluster by strain and the number of antigens recognized was comparable between the 2 strains of mice (Figure 5, G and H).

Together, these results suggest that the serum autoantibody response of lupus mice correlates to the classification paradigm. IgG autoantibodies in MRL/lpr mice have characteristics of an extrafollicular response (lower affinity, dominant IgG3 isotype, and broader antigen recognition profile), whereas the characteristics of IgG autoantibodies in NZB/W mice are consistent with a GC origin (higher affinity, lower frequency of IgG3, and more restricted antigen recognition profile). Interestingly, the IgM autoantibodies in NZB/W mice were similar to those in MRL/lpr mice in both affinity and antigen recognition profile, which may suggest that the IgM ANA$^+$ PCs, which are already present in young NZB/W mice, are of extrafollicular origin and that these may be unrelated to the emergence of IgG autoantibodies in older NZB/W mice that have characteristics of a GC origin.

Serum autoantibody characteristics correlate to classification of SLE patients. We next wanted to study whether autoantibody characteristics in SLE patients correlate to their classification, which may buttress the paradigm of a GC versus extrafollicular activation. We used hierarchical clustering to analyze whether a nonsupervised clustering would independently show a difference between the 2 clusters that we identified. When analyzing the ANA antigen specificity profile in serum IgG, we observed clustering of patients in accordance with our classification (Figure 6A). Serum IgG from cluster 1 patients recognized significantly more nuclear antigens than IgG from cluster 2 patients, similar to the difference we observed between MRL/lpr and NZB/W mice (characterized by an extrafollicular and GC differentiation pathways, respectively) (Figure 6B). In addition, we previously reported increased total ANA-IgG levels in MRL/lpr mice compared with NZB/W mice (2). Consistent with our paradigm, patients from cluster 1 also had higher titers of ANA-IgG in serum than patients in cluster 2 (Figure 6C). Likewise, although the number of patients with sufficient titers of anti-dsDNA to allow for determination of affinity was low, we observed a trend toward higher affinity in the patients from cluster 2 (Figure 6, D and E).

Importantly, the serum characteristics (number of nuclear antigens recognized and ANA-IgG titer) correlated most strongly with the relative proportion of ANA$^+$ PCs among ANA$^+$ antigen-experienced B cells (Supplemental Figure 2, A and D), rather than the frequency of ANA$^+$ or total PCs (Supplemental Figure 2, B, C, E, and F), further confirming that the classification paradigm we developed here, rather than simply the number of PCs, correlates to serum autoantibody characteristics and may thus correlate to an extrafollicular or GC response.

When including serology in the principal component analysis, the number of nuclear antigens that were recognized as well as total ANA-IgG in serum went in the same direction as PC frequencies and maintained the patient clusters (Figure 6, F and G). There are a few exceptions. One patient without PC expansion overlapped with cluster 1 on the initial principal component analysis based on flow cytometry data (Figure 1H); this patient also overlapped with patients from cluster 1 when ELISA data were included in the principal component analysis, and the antigen recognition profile of serum IgG resembled that of cluster 1 patients. Another exception is patient SLE 23, who was classified in cluster 2 in the first measurement but changed to cluster 1 upon a repeated measurement. Based on serology, this patient would classify as cluster 1. We did not include serology in the initial clustering, as serum was not available for all of our patients.

Discussion

In this study we observed distinct phenotypes of ANA$^+$ antigen-experienced B cells in patients with SLE. We propose that these reflect 2 pathways for PC differentiation, an extrafollicular pathway and a GC pathway. The stratification we propose may be relevant to other diseases with ANA autoantibodies (such as Sjögren's syndrome) or other autoantibodies, as several of these are heterogeneous diseases that have ectopic B cell activation that can represent GC or extrafollicular responses as well (28).

The first group of patients had no expansion of ANA$^+$ PCs compared with healthy controls. In addition, these patients clustered with healthy controls in principal component analysis. Several possible mechanisms could explain the absence of an abnormal B cell profile in these patients: (a) lower disease activity; (b) medication; (c) absence of current immune activation (there can be presence of autoantibody-producing PCs in the bone marrow without them being observed in the circulation); and (d) SLE pathogenesis caused by myeloid cell abnormalities rather than B cells. As we did not observe a lower disease activity or differences in medication of this group compared with the other groups, option 1 and 2 seem unlikely. Because these patients did not show any B cell abnormalities compared with healthy controls, we have not further analyzed them in this study.

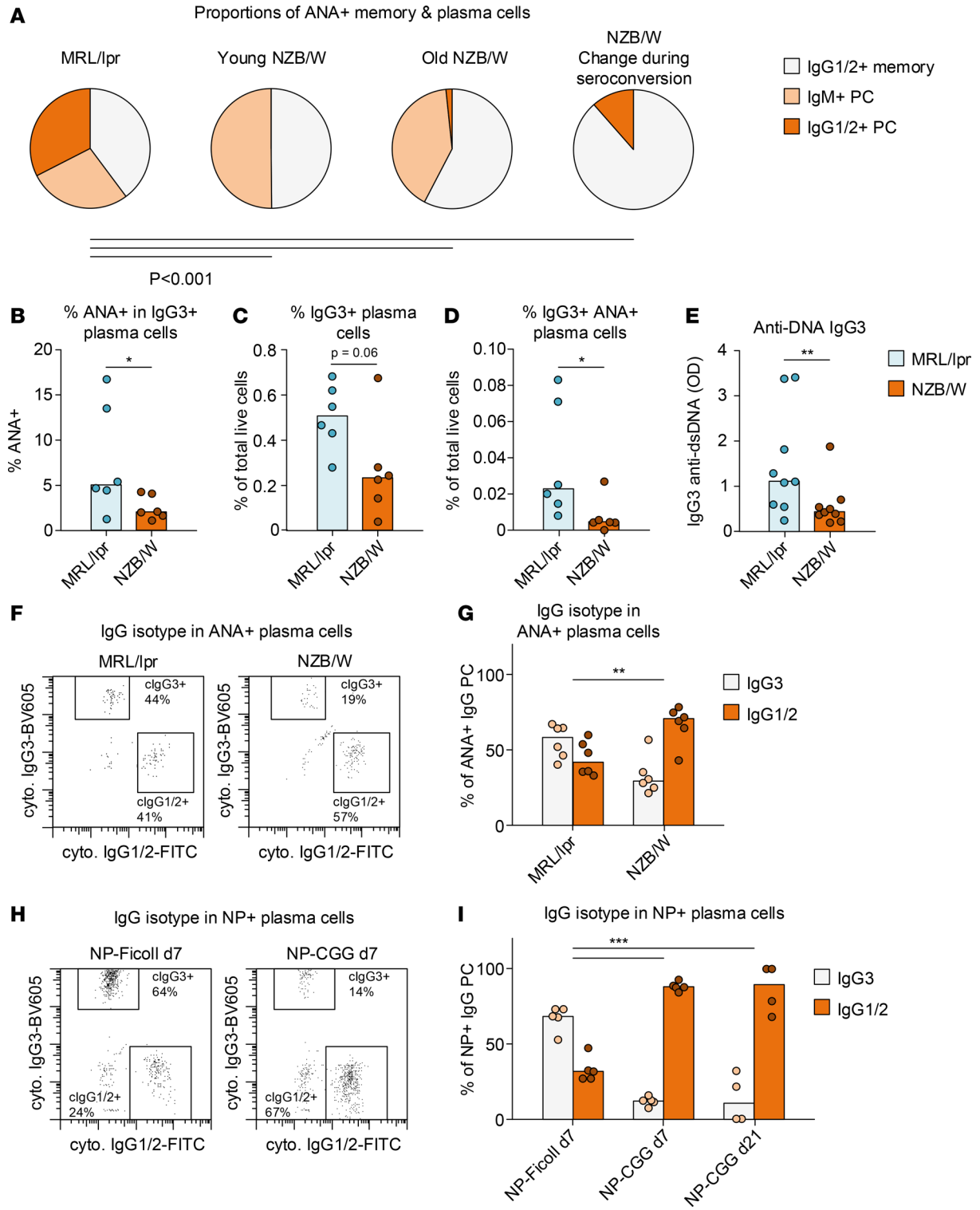

Figure 4. Frequencies of ANA⁺ memory B cells and PCs in MRL/lpr and NZB/W mice. (**A**–**G**) Splenocytes from MRL/lpr and NZB/W mice were stained with nuclear extract to analyze the percentage of ANA⁺ B cells. Each dot indicates an individual mouse (n = 5–8 for each group), and the bars represent the median. (**A**) Proportion of ANA⁺ antigen-experienced cells in the spleens of each mouse strain. NZB/W "Change during seroconversion" was calculated by subtracting the maximal measurements in young mice (quartile 3 + 1.5 × interquartile range) from the measurements in old mice. (**B**–**D**) The frequencies of total and ANA⁺ IgG3⁺ PCs. (**E**) dsDNA-reactive IgG3 in serum of MRL/lpr and NZB/W mice was determined by ELISA. (**F** and **G**) The relative number of IgG3⁺ and IgG1/2⁺ cells within the population of IgG ANA⁺ PCs of MRL/lpr and NZB/W mice. (**H** and **I**) The relative number of IgG3⁺ and IgG1/2⁺ cells within the population of IgM⁻ NP⁺ PCs of C57BL/6 mice immunized with NP-Ficoll (day 7) and NP-CGG (day 7 and day 21). $^*P < 0.05$; $^{**}P < 0.01$; $^{***}P < 0.001$, using χ^2 test (**A**), Mann Whitney U test (**B**–**E**), or 2-way ANOVA with Bonferroni post-hoc test (**G** and **I**). ANA, antinuclear antibody; CGG, chicken γ globulin; NP, 4-hydroxy-3-nitrophenylacetyl; PC, plasmablast/plasma cell.

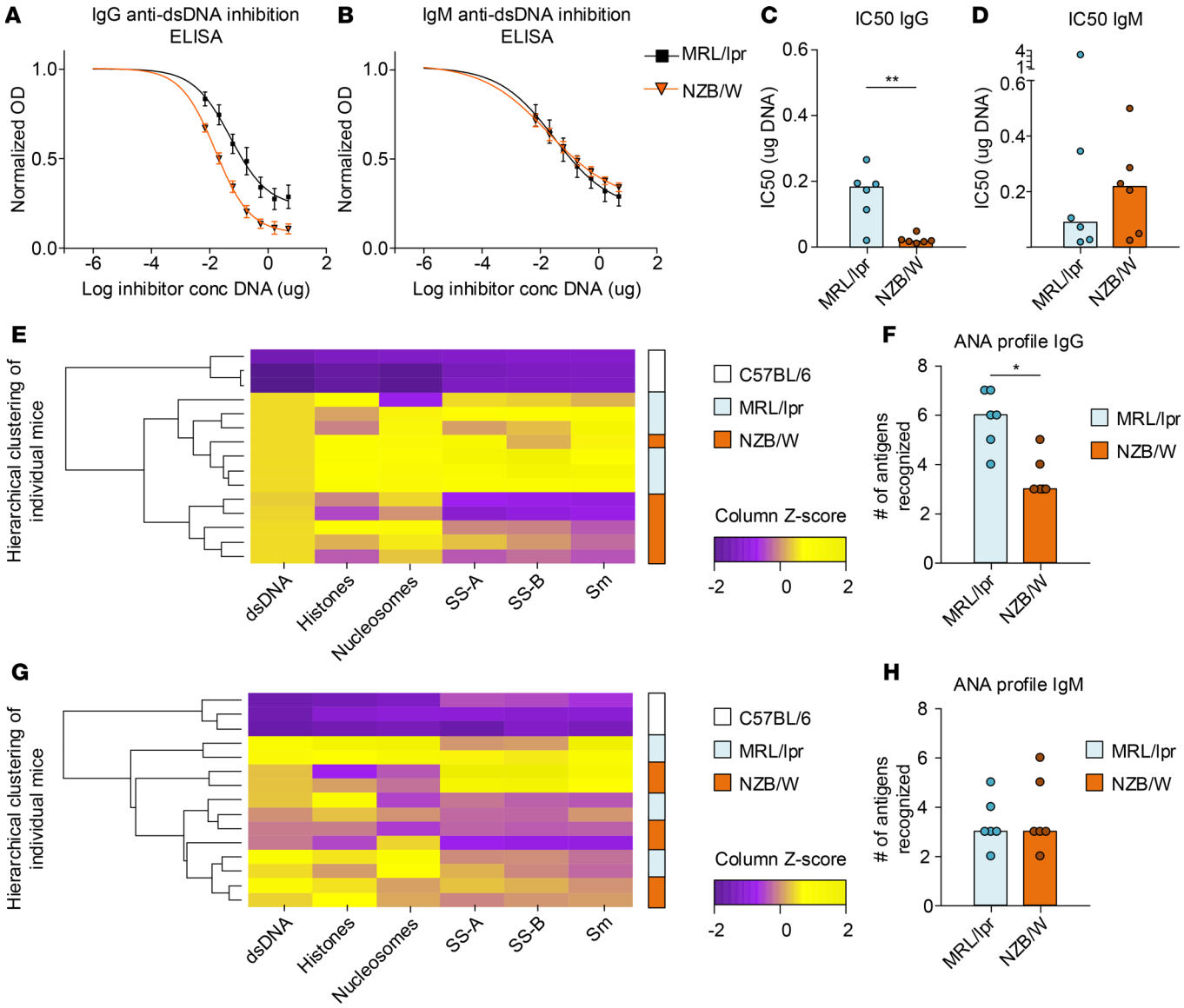

Figure 5. Characteristics of serum autoantibodies in lupus mice. (**A**–**D**) Relative affinity of anti-dsDNA IgG and IgM was measured in serum of MRL/lpr and NZB/W mice by inhibition ELISA. (**A** and **B**) Relative OD (average ± SEM) of each strain. (**C** and **D**) IC_{50} values for each individual mouse. (**E**–**H**) Profiles of recognition of nuclear antigens by serum IgG (**E** and **F**) and IgM (**G** and **H**). (**E** and **G**) Heatmaps, including hierarchical clustering based on the profile of antigen recognition. (**F** and **H**) The number of nuclear antigens recognized. Each dot indicates an individual mouse (n = 6–9 for each group), and the bars represent the median. *P < 0.05; **P < 0.01, using Mann Whitney U test. ANA, antinuclear antibody; cyto, cytoplasmic; PC, plasma cell; SS-A/B, anti–Sjögren's syndrome–related antigen; Sm, Smith antigen.

The second group of SLE patients (cluster 1) was characterized by a large number of ANA$^+$ PCs and reduced memory B cells, whereas the other group of patients (cluster 2) had a lower frequency of ANA$^+$ PCs (although still higher than healthy controls) and a higher frequency of ANA$^+$ memory B cells. Importantly, the clustering was not dependent on SLEDAI scores and was stable over time in the vast majority of patients, suggesting a way to subset SLE patients that is independent from disease activity. Similar frequencies (~20%) of patients with a plasmablast signature were found in another study of gene expression in pediatric SLE patients (29). This novel approach may have therapeutic implications. Although patients in cluster 1 were more frequently on steroids, this medication is associated with lower plasmablast gene signatures in blood (29) and reduces PC differentiation in vitro (30). Therefore, the phenotype we observed in cluster 1 (high frequency of ANA$^+$ PCs) is unlikely to be the consequence of treatment with steroids. It may be possible that patients in cluster 1 had a more intense medication scheme due to more cumulative disease activity (over the past few years) that was

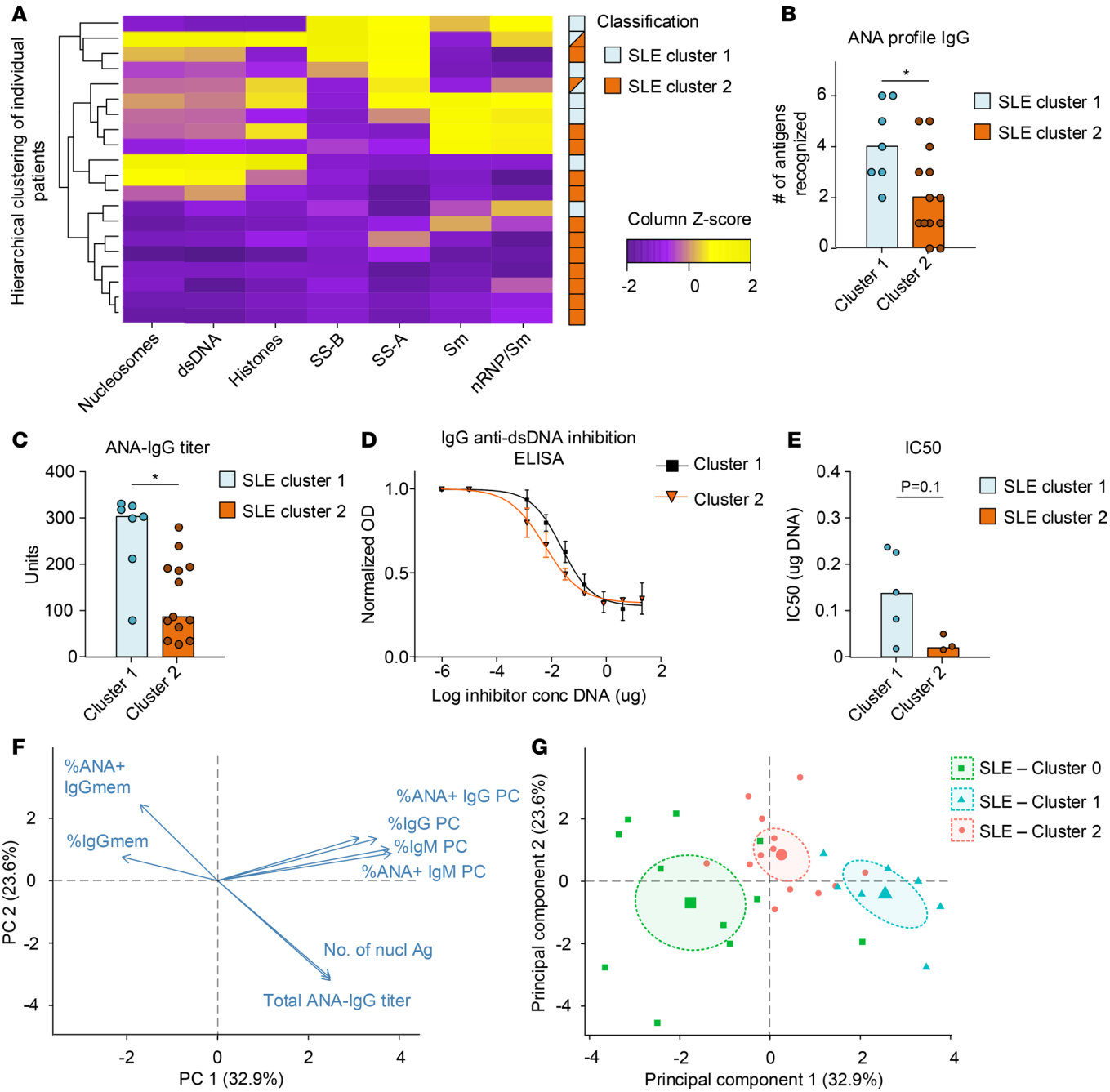

Figure 6. Characteristics of serum autoantibodies in SLE patients. (**A** and **B**) Profiles of recognition of nuclear antigens by serum IgG. Patients are separated based on classification, as described in Figure 1, into cluster 1 and cluster 2. (**A**) Heatmap, including hierarchical clustering based on the profile of antigen recognition. Blocks that show 2 colors represent the patients in which the classification changed over time (Figure 2), in which case the top left triangle represents the classification in the first measurement and the lower right represents the classification in the second measurement. (**B**) The number of nuclear antigens recognized. Each dot indicates an individual patient, and the bars represent the median. (**C**) Total ANA-IgG was determined by ELISA. (**D** and **E**) Relative affinity of anti-dsDNA IgG was measured in serum of SLE patients by inhibition ELISA. (**D**) Relative OD (average ± SEM) of each group is shown. (**E**) IC_{50} values for each individual patient. (**F** and **G**) Principal component analysis of all parameters analyzed (frequencies of ANA^+ and total B cell and PC subsets as well as ELISA recognition of nuclear antigens). The percentage indicated on the axis is the percentage of variance explained by that principal component. A selection of the vectors for direction of parameters is shown here. The parameters omitted here (ANA^+ and total transitional and naive B cells) are shown in Figure 1G. Their directionality remained the same. SLE patients were clustered as described in Figure 1. (**F**) The variables contributing to each dimension in principal component analysis. The length and direction of each arrow shows the strength of their contribution to each PC. (**G**) The coordinates of each SLE patient. Ellipses represent the 95% confidence interval for each group. *$P < 0.05$, using Mann Whitney *U* test. ANA, antinuclear antibody; PC, plasmablast/plasma cell; SS-A/B, anti–Sjögren's syndrome–related antigen; Sm, Smith antigen; SLE, systemic lupus erythematosus.

not directly reflected in current activity scores or clinical symptoms. This could also be related to a higher probability of patients in cluster 1 to experience clinical flares. A larger patient cohort with longitudinal data would be needed to confirm this.

We have correlated the relative frequencies of antigen-specific cells we observed in SLE patients to those in mice after primary immunization and in mice with lupus. The pattern we observed in patients from cluster 1 was comparable to extrafollicular immune activation during a primary immunization and to the pattern in MRL/lpr mice. The pattern we observed in patients from cluster 2 was comparable to GC immune activation and to the pattern in NZB/W mice. These data suggest that ANA^+ PCs in patients from cluster 1 derive from an extrafollicular pathway, whereas those in patients from cluster 2 may derive from a GC response. Importantly, the difference in several serum autoantibody characteristics (ANA titer, number of different antigens recognized, and affinity) between patients from each cluster further strengthens this notion. Literature suggests that extrafollicular autoreactive responses are characterized by higher autoantibody titers with lower affinity (31). Importantly, both extrafollicular and GC-derived autoantibodies led to similar kidney deposition and pathogenesis. This is in line with the data we present here in which patients from each cluster have comparable SLEDAI scores and renal involvement. Therefore, we believe that both extrafollicular and GC PC differentiation can lead to disease pathogenesis in SLE (32) and that our classification represents a simple way to stratify patients with respect to these pathways.

GC responses are well known to be increased in lupus-prone mice, and SLE patients often have increased numbers of circulating pre-GC B cells, switched memory B cells, and Tfh cells, suggestive of enhanced GC responses (8–10). Given that IgG anti-DNA autoantibodies that are considered to be pathogenic in SLE show evidence of SHM and often a loss of autoreactivity when reverted to the germline sequence (11), the production of autoreactive PCs by SHM of nonautoreactive naive B cells within the GC has been considered an important contributor to the development of SLE in both mice (12) and humans (13). Recent studies indicate the extrafollicular pathway also has a role in autoimmunity (6, 14, 15, 33). MRL/lpr mice exhibit extrafollicular PC generation, although they have increased formation of spontaneous GCs as well (8, 14, 16). Consistent with our results, two elegant studies by Sanz and colleagues have shown that activated naive B cells and age-associated B cells (ABCs) (designated DN2 in their study) can be clonally related to circulating PCs in SLE patients with active flares, and these may therefore derive from extrafollicular pathways (6, 33). In addition, Ettinger and colleagues have also shown a correlation of ABCs with disease activity, and in each study, the population also correlates with the frequency of PCs in SLE (34). Therefore, the extrafollicular pathway can be related to disease pathogenesis. However, the correlation to disease activity and PC frequencies is only evident when analyzing large patient numbers and is not dichotomous: Several patients have a high frequency of these cell subsets with a low disease activity and vice versa, suggesting that multiple pathways for disease pathogenesis exist. While neither group specifically proposed 2 pathways of PC differentiation, their data are consistent with the dichotomy we propose. Of the 5 patients Sanz and colleagues analyzed for activated naive cells, 2 exhibited more clonal relationships between PCs and naive cells, whereas the 3 other patients exhibited more clonal relationships between PCs and memory cells (6). Of the 8 patients they analyzed for switched ABCs, 3 had more clonal relationships between PCs and ABCs, whereas 4 had more clonal relationships between PCs and memory cells, and 1 additional patient had a comparable frequency of clonal relationships of PCs to ABCs and memory B cells (33). As they study primarily patients during a clinical flare, they may be observing a T-dependent response during the time of extrafollicular B cell activation prior to the GC response (Figure 1G). In any case, these data are in line with our hypothesis that SLE patients cluster in 2 groups based on distinct PC differentiation pathways that can be observed in circulating PCs.

Several studies have attempted to stratify SLE patients, most using gene expression profiles of peripheral leukocytes or subsets thereof, such as T cells or neutrophils (29, 35–37). Most of these studies have focused on correlations with disease activity or clinical symptoms, such as nephritis. These studies revealed correlations of plasmablast signatures and IFN signatures with disease activity in pediatric patients (29) and correlations of neutrophil signatures with lupus nephritis (29, 36). Two of these studies proposed stratification schemes based on the correlations of molecular parameters with SLEDAI score. In each scheme, the assignment of an individual patient to a cohort required longitudinal data (29, 36). Importantly, the correlations of specific groups of genes or signatures with disease activity suggest that different molecular pathways can contribute to active disease in patient groups, similar to what we propose here with respect to plasmablast derivation.

We believe the most important question is whether any proposed classification can identify those patients most likely to respond to a given therapeutic agent. Although providing novel insights into the heterogeneity of SLE, the stratifications proposed in the studies mentioned above often require multiple longitudinal measurements to determine patient clusters (29, 36), thereby limiting their applicability for stratifying patients going into clinical trials. While we currently cannot answer the question whether our classification will predict a response to particular therapy, this question can be addressed by using our methodology to analyze patients entering clinical trials with the methods we present. It is interesting to note that the mouse strains that we have described differ in their response to anti-IFN therapy, even though both strains have an IFN signature (38–40). It is likely that some therapeutic agents will preferentially target the GC PC differentiation pathway, while others will target the extrafollicular pathway. Classification of SLE patients by their PC differentiation pathway and then treating with an agent targeting that pathway should maximize the therapeutic response to a given agent and brings precision medicine to the lupus clinic.

Methods

Mice. C57BL/6, NZB/W F1, and MRL/lpr female mice were purchased from The Jackson Laboratory. Two- to six-month-old lupus-prone mice and age-matched controls were sacrificed at the time points indicated in Results, and bone marrow and spleens were obtained. For NP immunizations, C57BL/6 mice were immunized i.p. with 50 μg NP-AECM-Ficoll (at a conjugation ratio of 55:1) (Biosearch Technologies) in saline or with 100 μg NP-CGC (at a conjugation ratio of 20:1) (Biosearch Technologies) in alum (Thermo Fisher), after which spleens were obtained at day 7, 14, and 21. Single-cell suspensions were obtained from these tissues by standard procedures, and red blood cells were lysed using RBC lysis buffer (Biolegend). Serum from lupus-prone mice and their age-matched controls was obtained by submandibular bleeding.

SLE patients and healthy subjects. Blood from 36 SLE patients and 15 healthy subjects was collected in heparinized tubes, and PBMCs were obtained using standard Ficoll procedure. SLE diagnosis was based on 1997 revised ACR criteria (41). SLE patients receiving rituximab, belimumab, or cyclophosphamide in the preceding 12 months for the initial assessment were excluded from the study. One patient (SLE 32) used cyclophosphamide at the repeat measurement. At the time of the blood draw, all SLE patients were assessed for disease activity using the SLEDAI-2K (42). Patient characteristics are shown in Supplemental Tables 1 and 2.

Flow cytometry for ANA$^+$ B cells. Nuclear extract from HeLa cells was obtained as described previously (1). Briefly, nuclei from HeLa cells were isolated using the Nuclei EZ lysis kit (MilliporeSigma), fragmented by vortexing with 0.5-mm cell disruption glass beads (Scientific Industries), and biotinylated using EZ-Link-Sulfo-NHS-LC-biotin (Thermo Scientific). Staining for ANA$^+$ B cells was done as described previously (2). Briefly, cells were incubated with biotinylated nuclear extract in HBSS + 1.5% nonfat dry milk (LabScientific) for 30 minutes on ice. After thorough washing, cells were stained in HBSS + 2% FBS containing 1 μg/ml streptavidin-APC (Life Technologies) and cell surface antibodies. eFluor 506–labeled fixable viability dye (eBioscience) was added during staining with cell surface antibodies. For intracellular staining, cells were fixed and permeabilized with the Transcription Factor Staining Buffer Set (eBioscience) according to the manufacturer's instructions. After permeabilization, cells were stained in 1.5% nonfat dry milk (LabScientific) dissolved in permeabilization buffer with nuclear extract followed by streptavidin and anti-Ig antibodies dissolved in permeabilization buffer as described above.

The following anti-mouse antibodies were used: IgG1-FITC and -BV605 (clone A85-1), IgG2a,b-FITC and -BV605 (clone R2-40), IgG3-FITC and -BV605 (clone R40-82), IgD-PE (clone 11-26c.2a), and CD95-PECy7 (clone Jo2) (all from BD Biosciences); B220-PE-eF610 (clone RA3-6B2), IgM-eFluor450 (clone II/41), and GL7-FITC (clone GL7) (all from eBioscience); and CD3-BV510 (clone 17A2), CD19-BV711 (clone 6D5), and CD138-PE or -PerCpCy5.5 (clone 281-2) (all from Biolegend).

For staining of NP-specific B cells in immunized mice, NP-BSA-biotin (at a conjugation ratio of 6:1) (Biosearch Technologies) was preincubated for 30 minutes with streptavidin-APC in a 1:1 molar ratio, after which cells were incubated with 0.1 μg/ml NP-BSA-biotin + streptavidin-APC.

The following anti-human antibodies were used: IgG-FITC (G18-145, BD Biosciences); CD3-eF506 (UCHT1), CD14-eF506 (61D3), CD56-eF506 (TULY56), CD20-eF450 (2H7), CD38-PE-eF610 (HIT2), and CD27-PE (0323) (all from eBioscience); and CD19-PECy7 (HIB19) and IgM-PerCpCy5.5 (MHM-88) (both from Biolegend).

Flow cytometric acquisition was performed on Fortessa (BD). Analysis was performed using FACS Diva (BD) and FlowJo software.

We previously published the gating of our mouse and human B cell subsets (2). Briefly, gating was as follows for human B cells: transitional B cells were Dump$^-$ (FVD/CD3/CD14/CD56) CD19$^+$CD38^{++}CD27$^-$IgM^{++}; naive B cells were Dump$^-$CD19$^+$CD38$^+$CD27$^-$IgM$^{+/-}$IgG$^-$; IgM$^+$CD27$^+$ cells were Dump$^-$D19$^+$CD38$^{+/-}$CD27$^+$IgM$^+$IgG$^-$; IgG$^+$ memory cells were Dump$^-$CD19$^+$CD38$^{+/-}$CD27$^+$IgM$^-$IgG$^+$ and IgM$^+$; and IgG$^+$ PCs were Dump$^-$CD19$^+$CD20$^-$CD27^{++}CD38^{++} and cytoplasmic IgM$^+$IgG$^-$ or IgG$^+$IgM$^-$, respectively. Gating was as follows for mouse B cells: switched mIgG$^+$ B cells were FVD$^-$mIgG1/2a,b$^+$mIgM$^-$; IgG GC B cells were FVD$^-$B220$^+$IgG$^+$GL7^{++}CD95$^+$; IgG non-GC B cells were FVD$^-$B220$^+$IgG$^+$GL7$^-$; IgM$^+$ PCs were FVD$^-$B220^{lo}CD138$^+$cIgM^{++}cIgG$^-$; and IgG$^+$ PCs were FVD$^-$B220^{lo}CD138$^+$cIgG^{++}cIgM$^-$.

ELISA. Half-area 96-well ELISA plates (Corning) were coated with 400 μg/ml sonicated filtered calf-thymus DNA (Calbiochem). For analysis of binding to separate nuclear antigens, coated plates from the anti-ENA SLE profile-2 ELISA (Euroimmun) were used, combined with detection using AP-labeled anti-mouse IgM, IgG, or anti-human IgG (Southern Biotech). For analysis of total ANA-IgG titers in human samples, the Quanta Lite ANA ELISA (Inova diagnostics) was used, combined with detection using AP-labeled anti-human IgG (Southern Biotech).

Washing steps were performed with 0.05% Tween20 (Fisher) in PBS (Invitrogen). Plates were blocked with 1% BSA fraction V (Roche) in PBS for 1 hour at 37°C. Samples were diluted in 0.2% BSA in PBS, and incubated for 1.5 hours at 37°C. Serum samples were diluted ×40–×400 (depending on manufacturer's instructions). After washing, 1 μg/ml alkaline phosphatase–labeled goat anti-mouse IgM, total IgG, or IgG3 (Southern Biotech) was incubated for 1 hour at 37°C. For detection, 1 mg/ml phosphatase substrate (MilliporeSigma) was dissolved in substrate buffer (50 mM $NaHCO_3$, 1 mM $MgCl_2$; MilliporeSigma) for detection. The plates were read at 405 nm on a 1430 Multilabel Counter Spectrometer (PerkinElmer).

For inhibition ELISA to determine relative affinities of anti-dsDNA, plates were coated with 1 μg/ml calf thymus dsDNA (43). The EC_{50} was first established for each serum by performing serum titrations to ensure that the inhibition ELISA was performed in a linear range of the serum dilution. Subsequently, serum was diluted to the concentration equivalent to the EC_{50} and mixed with dsDNA, in 3-fold dilutions ranging from 5 to 0.0068 μg and 1 condition containing no dsDNA.

Statistics. Unless indicated otherwise, *P* values of less than 0.05 were considered statistically significant. Each experiment was performed at least twice to ensure reproducibility. For comparison of groups of mice or subjects, the Mann Whitney *U* test (2 tailed) was used. To compare frequencies, χ^2 test and Fisher exact test were used as indicated. To determine IC_{50} values for inhibition ELISAs, normalized OD values were calculated based on the maximum OD values when no inhibitor was present. Nonlinear regression [log(agonist) vs. response – variable slope] was used to interpolate the IC_{50} values at $Y = 0.5$. Correlations were calculated using Spearman's rank correlation.

Principal component analysis was performed using flow cytometry and ELISA data. Briefly, parameters were log transformed, scaled, and centered, after which principal components were calculated using prcomp. Principal components were visualized using the FactoExtra package. Heatmaps from ELISA data were generated using log-transformed OD values in the heatmap function. Heatmaps were scaled by column.

Statistical analysis was performed using GraphPad Prism 5 and R Studio 1.1.

Study approval. Mice were housed in according to AAALAC regulations, and all mouse studies were approved the Institutional Animal Care and Use Committee of the Feinstein Institute for Medical Research. The study with SLE patients and healthy subjects was approved by the Northwell Health Institutional Review Board, and all subjects gave written informed consent.

Author contributions

JS and BD designed research studies and wrote the manuscript. JS, YAF, ANB, SAC, MCM, and CA conducted experiments. JS and YAF analyzed data.

Acknowledgments

We thank Heriberto Borrero and Chris Colon (flow cytometry core facility, Feinstein Institute for Medical Research) for their support in flow-assisted cell sorting. JS received financial support from the American Autoimmune Related Disease Association. This work was further supported by NIH grant 1P01 AI073693.

Address correspondence to: Betty Diamond, Center of Autoimmune Musculoskeletal and Hematopoietic Diseases, Feinstein Institute for Medical Research, 350 Community Drive, Manhasset, New York 11030, USA. Phone: 516.562.3830; Email: bdiamond@northwell.edu.

1. Malkiel S, et al. Checkpoints for autoreactive B cells in the peripheral blood of lupus patients assessed by flow cytometry. *Arthritis Rheumatol*. 2016;68(9):2210–2220.
2. Suurmond J, et al. Loss of an IgG plasma cell checkpoint in patients with lupus. *J Allergy Clin Immunol*. 2019;143(4):1586–1597.
3. Scheid JF, Mouquet H, Kofer J, Yurasov S, Nussenzweig MC, Wardemann H. Differential regulation of self-reactivity discriminates between IgG$^+$ human circulating memory B cells and bone marrow plasma cells. *Proc Natl Acad Sci U S A*. 2011;108(44):18044–18048.
4. Tiller T, Tsuiji M, Yurasov S, Velinzon K, Nussenzweig MC, Wardemann H. Autoreactivity in human IgG$^+$ memory B cells. *Immunity*. 2007;26(2):205–213.
5. Wardemann H, Yurasov S, Schaefer A, Young JW, Meffre E, Nussenzweig MC. Predominant autoantibody production by early human B cell precursors. *Science*. 2003;301(5638):1374–1377.
6. Tipton CM, et al. Diversity, cellular origin and autoreactivity of antibody-secreting cell population expansions in acute systemic lupus erythematosus. *Nat Immunol*. 2015;16(7):755–765.
7. Vinuesa CG, Sanz I, Cook MC. Dysregulation of germinal centres in autoimmune disease. *Nat Rev Immunol*. 2009;9(12):845–857.
8. Luzina IG, et al. Spontaneous formation of germinal centers in autoimmune mice. *J Leukoc Biol*. 2001;70(4):578–584.
9. Arce E, Jackson DG, Gill MA, Bennett LB, Banchereau J, Pascual V. Increased frequency of pre-germinal center B cells and plasma cell precursors in the blood of children with systemic lupus erythematosus. *J Immunol*. 2001;167(4):2361–2369.
10. Zhang X, et al. Circulating CXCR5$^+$CD4$^+$ helper T cells in systemic lupus erythematosus patients share phenotypic properties with germinal center follicular helper T cells and promote antibody production. *Lupus*. 2015;24(9):909–917.
11. Brink R. The imperfect control of self-reactive germinal center B cells. *Curr Opin Immunol*. 2014;28:97–101.
12. Guo W, Smith D, Aviszus K, Detanico T, Heiser RA, Wysocki LJ. Somatic hypermutation as a generator of antinuclear antibodies in a murine model of systemic autoimmunity. *J Exp Med*. 2010;207(10):2225–2237.
13. Mietzner B, et al. Autoreactive IgG memory antibodies in patients with systemic lupus erythematosus arise from nonreactive and polyreactive precursors. *Proc Natl Acad Sci U S A*. 2008;105(28):9727–9732.
14. William J, Euler C, Christensen S, Shlomchik MJ. Evolution of autoantibody responses via somatic hypermutation outside of germinal centers. *Science*. 2002;297(5589):2066–2070.
15. Deng R, et al. Extrafollicular CD4. *Nat Commun*. 2017;8(1):978.
16. Odegard JM, et al. ICOS-dependent extrafollicular helper T cells elicit IgG production via IL-21 in systemic autoimmunity. *J Exp Med*. 2008;205(12):2873–2886.
17. Grammer AC, et al. Abnormal germinal center reactions in systemic lupus erythematosus demonstrated by blockade of CD154-CD40 interactions. *J Clin Invest*. 2003;112(10):1506–1520.
18. Weisel FJ, Zuccarino-Catania GV, Chikina M, Shlomchik MJ. A Temporal switch in the germinal center determines differential output of memory B and plasma cells. *Immunity*. 2016;44(1):116–130.
19. Shinnakasu R, et al. Regulated selection of germinal-center cells into the memory B cell compartment. *Nat Immunol*. 2016;17(7):861–869.
20. Ise W, et al. T follicular helper cell-germinal center B cell interaction strength regulates entry into plasma cell or recycling germinal center cell fate. *Immunity*. 2018;48(4):702–715.e4.
21. Sweet RA, Christensen SR, Harris ML, Shupe J, Sutherland JL, Shlomchik MJ. A new site-directed transgenic rheumatoid factor mouse model demonstrates extrafollicular class switch and plasmablast formation. *Autoimmunity*. 2010;43(8):607–618.
22. Huang W, et al. BAFF/APRIL inhibition decreases selection of naive but not antigen-induced autoreactive B cells in murine systemic lupus erythematosus. *J Immunol*. 2011;187(12):6571–6580.
23. Chang NH, MacLeod R, Wither JE. Autoreactive B cells in lupus-prone New Zealand black mice exhibit aberrant survival and proliferation in the presence of self-antigen in vivo. *J Immunol*. 2004;172(3):1553–1560.
24. Hess C, et al. T cell-independent B cell activation induces immunosuppressive sialylated IgG antibodies. *J Clin Invest*. 2013;123(9):3788–3796.
25. Snapper CM, et al. Induction of IgG3 secretion by interferon gamma: a model for T cell-independent class switching in response to T cell-independent type 2 antigens. *J Exp Med*. 1992;175(5):1367–1371.
26. Takahashi S, Nose M, Sasaki J, Yamamoto T, Kyogoku M. IgG3 production in MRL/lpr mice is responsible for development of lupus nephritis. *J Immunol*. 1991;147(2):515–519.
27. Greenspan NS, et al. IgG3 deficiency extends lifespan and attenuates progression of glomerulonephritis in MRL/lpr mice. *Biol Direct*. 2012;7:3.
28. Szyszko EA, Brokstad KA, Oijordsbakken G, Jonsson MV, Jonsson R, Skarstein K. Salivary glands of primary Sjögren's syndrome patients express factors vital for plasma cell survival. *Arthritis Res Ther*. 2011;13(1):R2.
29. Banchereau R, et al. Personalized immunomonitoring uncovers molecular networks that stratify lupus patients. *Cell*. 2016;165(3):551–565.
30. Haneda M, Owaki M, Kuzuya T, Iwasaki K, Miwa Y, Kobayashi T. Comparative analysis of drug action on B-cell proliferation and differentiation for mycophenolic acid, everolimus, and prednisolone. *Transplantation*. 2014;97(4):405–412.
31. Kim SJ, et al. Increased IL-12 inhibits B cells' differentiation to germinal center cells and promotes differentiation to short-lived plasmablasts. *J Exp Med*. 2008;205(10):2437–2448.
32. Malkiel S, Barlev AN, Atisha-Fregoso Y, Suurmond J, Diamond B. Plasma cell differentiation pathways in systemic lupus erythematosus. *Front Immunol*. 2018;9:427.
33. Jenks SA, et al. Distinct effector B cells induced by unregulated toll-like receptor 7 contribute to pathogenic responses in systemic lupus erythematosus. *Immunity*. 2018;49(4):725–739.e6.

34. Wang S, et al. IL-21 drives expansion and plasma cell differentiation of autoreactive CD11c. *Nat Commun*. 2018;9(1):1758.
35. Bradley SJ, Suarez-Fueyo A, Moss DR, Kyttaris VC, Tsokos GC. T cell transcriptomes describe patient subtypes in systemic lupus erythematosus. *PLoS One*. 2015;10(11):e0141171.
36. Toro-Dominguez D, Martorell-Marugan J, Goldman D, Petri M, Carmona-Saez P, Alarcon-Riquelme ME. Stratification of systemic lupus erythematosus patients into three groups of disease activity progression according to longitudinal gene expression. *Arthritis Rheumatol*. 2018;70(12):2025–2035.
37. Ding Y, et al. Identification of a gene-expression predictor for diagnosis and personalized stratification of lupus patients. *PLoS One*. 2018;13(7):e0198325.
38. Zhou Z, et al. Phenotypic and functional alterations of pDCs in lupus-prone mice. *Sci Rep*. 2016;6:20373.
39. Mathian A, Weinberg A, Gallegos M, Banchereau J, Koutouzov S. IFN-α induces early lethal lupus in preautoimmune (New Zealand Black x New Zealand White) F1 but not in BALB/c mice. *J Immunol*. 2005;174(5):2499–2506.
40. Schwarting A, et al. Interferon-β: a therapeutic for autoimmune lupus in MRL-Faslpr mice. *J Am Soc Nephrol*. 2005;16(11):3264–3272.
41. Hochberg MC. Updating the American College of Rheumatology revised criteria for the classification of systemic lupus erythematosus. *Arthritis Rheum*. 1997;40(9):1725.
42. Gladman DD, Ibañez D, Urowitz MB. Systemic lupus erythematosus disease activity index 2000. *J Rheumatol*. 2002;29(2):288–291.
43. Rath S, Stanley CM, Steward MW. An inhibition enzyme immunoassay for estimating relative antibody affinity and affinity heterogeneity. *J Immunol Methods*. 1988;106(2):245–249.